0273-2289/88/1700-0055/$03.60

Effect of Diffusion in Solid Acid Catalyzed Inulin Hydrolysis

S. B. KIM AND Y. Y. LEE*

Department of Chemical Engineering, Auburn University, AL 36849

ABSTRACT

Hydrolysis of inulin was investigated employing various solid acids as hydrolytic catalysts. The catalytic performances of several ion exchange resins were compared. The effects of the particle size and porosity on the hydrolysis reaction were found to be significant, indicating that the intraparticle diffusion of reactants controls the reaction rate. Theoretical models were developed, therefore, to analyze the effects of intraparticle diffusion occurring in a sequential reaction. The results were found to be consistent with experimental observations regarding the adverse effects of pore diffusion and the reaction pattern.

Index Entries: Inulin; hydrolysis; ion-exchange-resin; intra-particle-diffusion.

INTRODUCTION

Fructose is a natural sugar reported to have 1.5 to 2 times the sweetness of sucrose. As a sweetener, fructose carries some unique and desirable characteristics (*1*), and the demand for it has increased significantly in recent years. Currently, fructose syrups are produced mainly by enzymatic hydrolysis of starch to glucose and subsequent isomerization. Further separation is also required to make it into a high grade form (*2*).

Hydrolysis of inulin is a feasible alternative approach applicable for production of high grade fructose. Polyfructans with a degree of polymerization of at least 30 are commonly referred to as inulin. This natural carbohydrate exists in easily recoverable form in various plants, including Jerusalem artichoke, chicory, and dahlia. For hydrolysis of polyfructans, free acid catalysts have been applied in the past with limited suc-

*Author to whom all correspondence and reprint requests should be addressed.

cess, the main drawback being significant decomposition of fructose (*3–7*). As a hydrolytic catalyst, solid acids have several advantages over free acids (*8*): Solid acids are easily recoverable; the product is free of residual acid, a contaminant; the reaction environment is corrosion-free. Our previous study along this line has also shown that the hydrolysis of sugar oligomers by solid acid produces much less sugar decomposition products in comparison to a straight acid process (*9*).

On the other hand, hydrolysis of polyfructans involves a sequential reaction (hydrolysis and decomposition) and it occurs in the pores of the catalyst matrix, which brings about a potential adverse effect linked with diffusion in porous media. The diffusional effects concerning ion exchange resin catalysts have indeed been reported in esterification of butanol and oleic acid (*10*) as well as hydrolysis reactions of various types (*11–15*). However, we find the nature of these studies quite different from inulin hydrolysis and inappropriate for direct application in that the reactants involved in these reactions had much smaller molecular weight than inulin, and the decomposition part of the reaction was disregarded.

The purpose of this study was to assess the performance of cation resins as catalysts in inulin hydrolysis. Since this process presented a unique and rather complicated situation regarding the kinetics, reaction pattern, and the diffusion phenomena, a considerable portion of this study was devoted for interpretation of experimental data by mathematical means focusing on the mass transfer effects.

THEORETICAL

Catalyst Selectivity in Consecutive Reactions

Diffusion of reactants and products within porous resin particles can significantly affect catalyst selectivity when the desired product is the intermediate component in a sequential reaction. Wheeler appears to have been the first to examine this situation mathematically (*16*).

The kinetics of inulin hydrolysis is represented by the consecutive first order reactions of

$$A \xrightarrow{1} B \xrightarrow{2} C$$

where A is inulin; B, fructose; and C, HMF and other decomposition products.

Further assumptions are made in the modeling procedure. Diffusion resistance of the reactants and products across the external film is negligible. The shape of the resin particle is represented by a flat plate.

Two types of catalysts, i.e., nonporous catalyst and porous catalyst, were examined in this study.

Nonporous Catalyst

For a nonporous catalyst, bulk concentrations of *A* and *B* at a point in the reactor are the same as those at the catalyst surface. The reaction rates on components *A* and *B* are therefore expressed by the following differential equations.

$$-dC_{Ab}/dt = k_1 C_{Ab} \quad (1)$$

$$dC_{Bb}/dt = k_1 C_{Ab} - k_2 C_{Bb} \quad (2)$$

By dividing Eq. [2] by Eq. [1] and integrating the resulting equation with conditions $C_{Ab} = C_{Ao}$ and $C_{Bb} = 0$, the following solution is obtained.

$$C_{Bb}/C_{Ao} = -(S/(S-1))(C_{Ab}/C_{Ao})(1-(C_{Ab}/C_{Ao})^{1/S-1}) \quad (3)$$

where $S = k_1/k_2$
C_{Ab}, C_{Bb} = bulk concentrations of A and B, respectively
C_{Ao} = initial concentration

Porous Catalyst

Unsteady State Model

A material balance on component *A* and *B* within a differential =segment of catalyst yields the following equations

$$De_A\, d^2C_A/dx^2 - (-r_A) = 0 \quad (4)$$

$$De_B\, d^2C_B/dx^2 + r_B = 0 \quad (5)$$

where De_A and De_B are effective diffusivities of *A* and *B*, respectively, and were assumed to remain constant during the reaction. In a strict sense, this assumption is incorrect, since *DP* of polyfructans decreases as reaction progresses. Furthermore the feed contains a mixture of fructans with varying *DP*s. As a practical solution an average value of diffusivity can be applied. The boundary conditions are

$$\text{at } x = 0,\ C_A = C_{As} \quad (6)$$

$$C_B = C_{Bs} \quad (7)$$

$$\text{at } x = L,\ dC_A/dx = 0 \quad (8)$$

$$dC_B/dx = 0 \quad (9)$$

where C_{As} and C_{Bs} are concentrations of *A* and *B* at the catalyst surface, respectively, and vary as reaction progresses. The boundary conditions [8] and [9] indicate that there is a symmetry formed in concentration profile at $x = L$, the center point of catalyst. The solution to Eq. [4] with boundary conditions [6] and [8] is as follows.

$$C_A/C_{As} = \cosh \phi(1-x/L)/\cosh \phi \quad (10)$$

By substituting Eq. [10] into Eq. [5] and integrating the resulting equation with boundary conditions [7] and [9], one obtains the following solution.

$$C_B/C_{BS} = [1 - C_{AS}S/C_{BS}(1 - SR_D)][\cosh((1 - x/L)\phi/Y)/\cosh(\phi/Y)] + [C_{AS}S/C_{BS}(1 - SR_D)][\cosh(\phi(1 - x/L))/\cosh\phi] \quad (11)$$

where $\phi^2 = k_1L^2/De_A$

$R_D = De_B/De_A$

$Y = (SR_D)^{.5}$

The main interest of this analysis is in the integrated yield of B for the entire catalyst, i.e., the net of mol of *B* that flows out of the catalyst divided by the mol of *A* that flows in. The integrated yield of *B* is then calculated by the ratio of the concentration gradients of *A* and *B* at the catalyst surface. The rate of disappearance of *A* within the catalyst must be equal to the net rate of diffusion into the catalyst, such that

$$(-r_A)_{x=0} = -ADe_A(dC_A/dx)_{x=0} \quad (12)$$

The rate of production of *B* can also be described in a similar manner.

$$(r_B)_{x=0} = -ADe_B(dC_B/dx)_{x=0} \quad (13)$$

The terms, (dC_A/dx) and (dC_B/dx), in Eqs. [12] and [13] can be obtained by differentiating Eqs. [10] and [11] at $x = 0$. The ratio of the production rate of *B* and the disappearance rate of *A* is expressed by

$$-(dC_{BS}/dC_{AS})_{x=0} = R_D[(S/(SR_D-1)) - (C_{BS}/C_{AS} + S/(SR_D-1))(1/Y)(\tanh(\phi/Y)/\tanh\phi)] \quad (14)$$

Integration of Eq. [14] with condition $C_{Bs} = 0$ at $C_{As} = C_{Ao}$ gives

$$C_{Bb}/C_{Ao} = [S(R_D-K)/(SR_D - 1)(1 - K)](C_{Ab}/C_{Ao})[(C_{Ab}/C_{Ao})^{K-1} - 1] \quad (15)$$

where $K = (R_D/S)^{.5}\tanh\phi/Y/\tanh\phi$

If there is no diffusional resistance (i.e., $\phi = 0$), Eq. [15] converts exactly to Eq. [3].

Pseudo Steady State Model

In the analysis to this point, the effect of diffusion on yield of desired product has been studied without involving the time variable by dividing one rate equation by another. To study the reaction conversion as function of time, a pseudo steady state assumption was introduced. This assumption disregards the partial derivative with respect to time in the material balance inside the pores of the solid particles, as indicated by Eq. [16].

$$\partial C_A/\partial t = \partial C_B/\partial t = 0 \quad (16)$$

In practical terms, it means that the concentration profile within the solid particle conforms to Eqs. [10] and [11] at all time even though the external concentration is gradually changing. This assumption is valid if the amount of liquid retained in catalyst is much smaller than the amount of bulk liquid, which has been the case in this study. Then the following equations are obtained for a batch reactor system.

$$V\, dC_{Ab}/dt = De_A A(dC_A/dx)_{x=0} \quad (17)$$

$$V\, dC_{Bb}/dt = De_B A(dC_B/dx)_{x=0} \quad (18)$$

where V = reactor volume
A = total external surface area of catalyst

Eqs. [17] and [18] indicate that the time variations of A and B in a batch reactor must be equal to the net rate of diffusion of A and B at the catalyst surface. By differentiating Eqs. [10] and [11] with respect to x at $x = 0$, and substituting the resulting terms into Eqs. [17] and [18], one obtains

$$V\, dC_{Ab}/dt = -De_A(A/L)\,(C_{Ab}\,\phi \sinh \phi/\cosh \phi) \quad (19)$$

$$V\, dC_{Bb}/dt = De_B(A/L)\,[(C_{Ab}S/(1 - SR_D) - (Bb)(J \sinh J/\cosh J) - C_{Ab}S/(1 - SR_D)\,(\phi \sinh \phi/\cosh \phi)] \quad (20)$$

where $J = \phi/Y$

EXPERIMENTAL

Materials

Inulin from Dahlia tubers (Sigma Chemical) was used as the substrate. The inulin samples were dissolved into distilled water to 5.5% w/v, and demineralized by treating with cation and anion resins. The pH and specific conductivities of the final solution after treatment were 4.5 and 10 μmos/cm^3, respectively. The cation resins used as catalysts were Nafion 1200 EW, Amberlite 118H, 120-P and 200, and Dowex 50Wx2-100, 50Wx2-200, 50Wx2-400, 50Wx4-100, 50Wx8-100, and 50Wx12-100, the last suffix in Dowex indicating the nominal mesh size.

Reaction

Batch reactions were carried out in a flash (125 mL) equipped with a reflux condenser under constant temperature. Mild agitation just enough to suspend the resin was applied. The resin concentration used ranged from .0375–.05 g wet resin/mL of solution. Samples were taken through a 60 μm filter.

For studies involving continuous reaction, a reactor setup described in our previous study was used (*9*). In this case, a stainless steel tubular reactor having 57 mL capacity was used as a continuous integral reactor.

Diffusivity

Diffusivities of fructose and inulin were measured by studying the unsteady state sorption phenomena by cation exchange resins. In the procedure, the cation exchange resin was carefully blotted dry with filter paper to remove all surface moisture after washing with deionized water several times and separating from the water by filtration. Ten g of it was poured into a beaker containing 80 mL of 5% fructose or inulin solution. Liquid samples were taken periodically and analyzed. The unsteady state sorption rates of fructose and inulin were employed in a statistical analysis designed to determine the effective diffusivities. The classical solution for unsteady state diffusion in a sphere given by Crank (*17*) was utilized in this statistical parameter estimation procedure.

Analysis

The fructose and inulin contents were determined by HPLC equipped with a refractive index detector (Waters Associate). The column contained Bio-Rad Q15S ion exchange resin in calcium form. The HMF contents were measured by the same HPLC unit using a UV detector (Varian Aerograph 8055) set at 254 nm.

RESULTS AND DISCUSSION

Performance of Various Solid Acids

The cation exchange resins used in the initial hydrolysis tests include Nafion, Dowex 50Wx2-100, Amberlite 200, 118H, and 120-P. Some of the important characteristics of these resins are shown in Table 1. The experiments were conducted using a continuous integral plug flow reactor at 90°C. The catalyst particles were packed into the reactor such that the packing density was about .75 g dry resin/mL reactor. The reactor voidage was .28. A constant volumetric loading of 57 mL of wet resin/reactor was applied for all catalysts. Figure 1 shows the reaction progress as function of reactor residence time for each catalyst. Dowex 50x2-100 exhibited the highest specific catalyst activity among the resins used in this study. The maximum attainable fructose yield was achieved in 20 min of residence time. Contributing to the high activity of Dowex resin were its small particle size and low degree of crosslinkage. Amberlite 200, a macroreticular type resin, was found to be only slightly less active than Dowex resin. Amberlite 200 has a macroporous structure with high porosity (36%) and large pore size (80 A average) (*19*), whereas the gel type resins typically have 10–20 A pore size (*20*). The high porosity and pore size would be a desirable feature in dealing with reactants having large molecular size because it allows easy penetration into the resin. On the other hand, it may reduce the ionic capacity of the resin. Amberlite IRA-118H gave the lowest fructose yield and highest HMF concentration

Table 1
Characteristics of Ion Exchange Resins

Resin	Type	Crosslinkage, %	Wet Mesh	Capacity, meq/dry g	Max. operating temp., C
Dowex 50x2-100	gel	2	50–100[a]	5.3	150
Amberlite 200	macroreticular	20	16–50	4.3	150
Amberlite IRA-118H	gel	4.5	16–50	4.9	120
Amberlite 120-P	gel	8	16–50	4.4	120
Nafion	gel	uncrosslinked	60–100[a]	.8	250

[a]Indicates dry mesh.

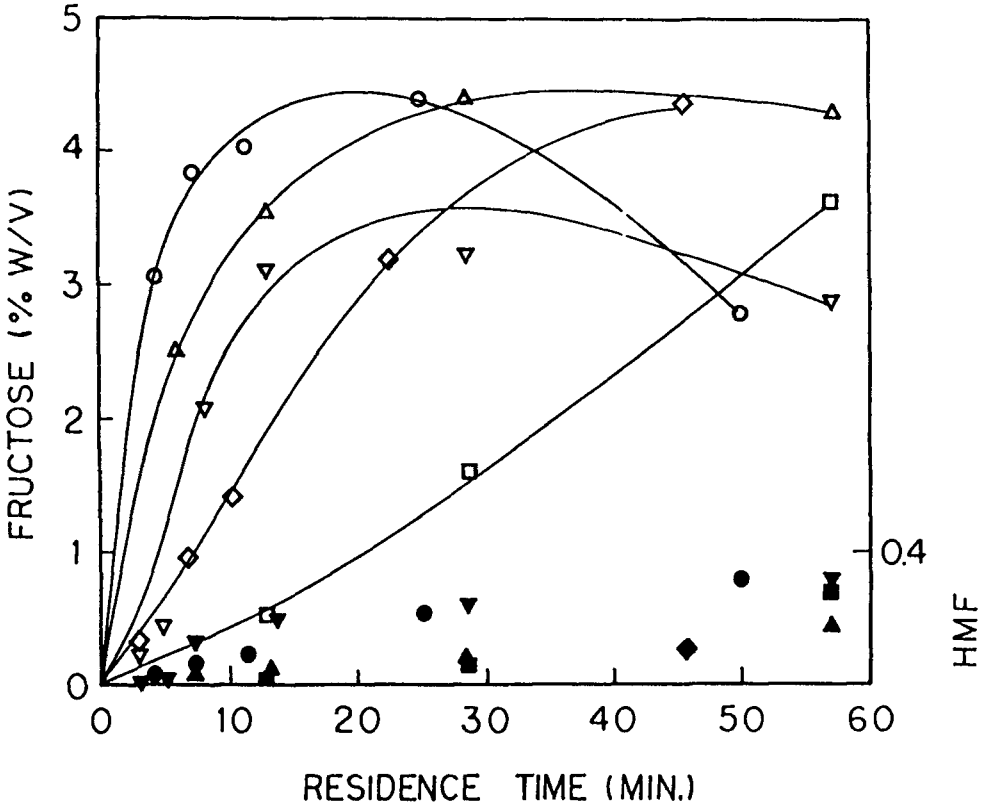

Fig. 1. Reaction progression in inulin hydrolysis by various ion exchange resins. Integral plug flow reactor. 90°C. Filled Symbol: HMF. (○● Dowex 50x2-100; △▲ Amberlite 200; ◇◆ Nafion; ▽▼ Amberlite 118H; □■ Amberlite 120-P).

at the initial stage of reaction. Nafion showed a low catalytic activity because of its low ion capacity, but it also produced low HMF, indicating the selectivity index (hydrolysis/decomposition) may be as high as those of Dowex and Amberlite 200. Amberlite 120-P had the lowest catalytic activity. In the last three cases, a peculiar reaction pattern was observed that the reaction was particularly slow at the initial stage. This feature will be discussed in the latter section of this paper. The results obtained thus far indicate that Dowex 50Wx2-100 and Amberlite 200 are the most suitable catalysts among the five investigated in terms of catalytic activity and HMF formation. For these two resins, the maximum operating temperature is 150°C. The specific activity can be enhanced quite substantially by raising the reaction temperature beyond the level of 90°C applied in this study. This point is particularly meaningful in the case of Nafion, which is extremely heat stable with the upper bound operating temperature of 250°C. In other words, the low reactivity of Nafion can easily be compensated by elevation of the reaction temperature. This reasoning and the fact that Nafion gave the lowest degree of sugar decomposition would make it an acceptable catalyst for inulin hydrolysis.

Effect of Particle Size and Porosity

In the foregoing study, it was evident that the particle size and porosity of resin significantly affect the hydrolysis reaction of inulin. To investigate this matter more closely, further experiments were carried out employing three different particle sizes of Dowex 50W resins (dry mesh 50–100, 100–200, and 200–400 with the same crosslinkage, 2%). The reactions were carried out in a stirred batch reactor at 100°C. Catalyst loading was 3 g dry resin/80 mL of inulin solution. Figure 2 illustrates the effect of particle size on reaction rate. It is quite clear that the reaction rate increased as the particle size decreased, indicating that only acid groups at or near the surface of a resin particle are effective, or that intraparticle diffusion controls the reaction rate.

Porosity of an ion exchange resin in general has an inverse relationship with the degree of crosslinkage such that low crosslinkage induces high porosity. A resin with a low degree of crosslinking therefore tends

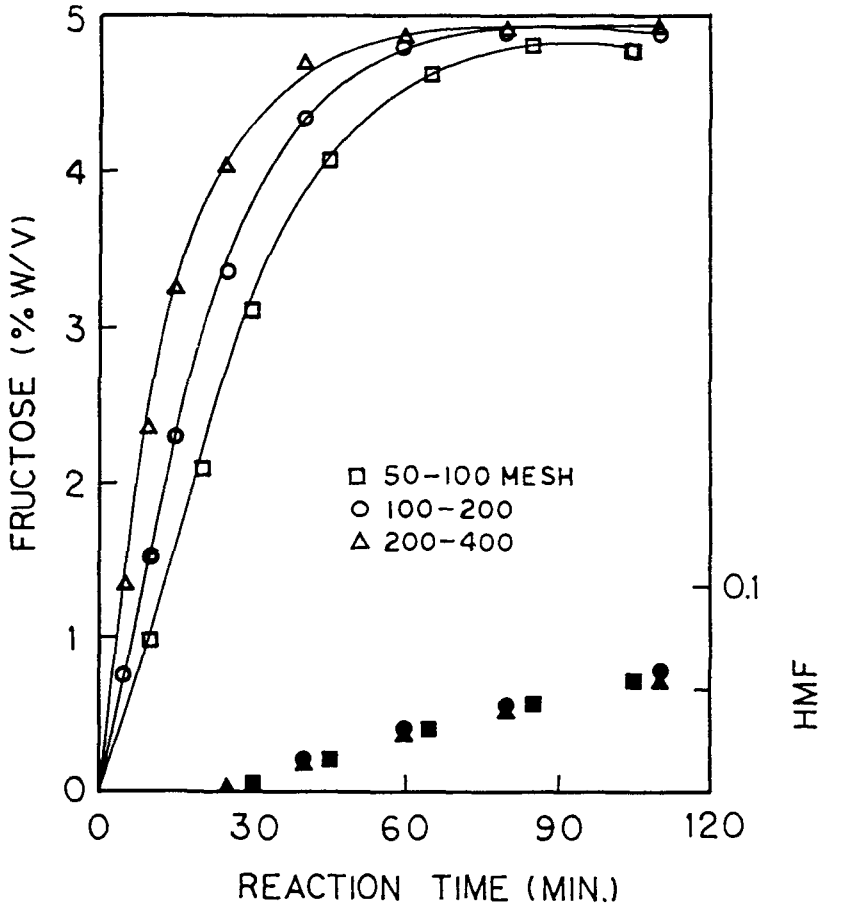

Fig. 2. Effect of particle size on reaction rate (2% crosslinkage). Dowex 50Wx2 resins. Batch reactor. 100°C. Catalyst loading: 3 g/80 mL. Filled Symbols: HMF.

to render high permeability for reactants. Figure 3 shows such effect as applied to Dowex 50W resins. It is clearly seen that the reaction rate increased significantly with decreasing degree of crosslinking, reaffirming the presence of strong diffusional effect. Although the dry mesh sizes of resins were identical for each case, size variation of resin has occurred because of differences in swelling factor. For example, the size of 2% crosslinked resin (swelling factor = 1.9) was actually larger than that of 12% crosslinked resin (swelling factor = 1.35) (*21*).

Also noticeable from Fig. 3 is that the terminal HMF production increased as the particle size and crosslinking increased, indicating that the pore diffusion affects not only the rate of reaction but also the selectivity. This observation became an impetus for the theoretical part of this investigation.

Unsteady State Model

The effect of intraparticle diffusion on the yield of desired product (*B*) in the consecutive reaction (A→B→C) was examined according to the

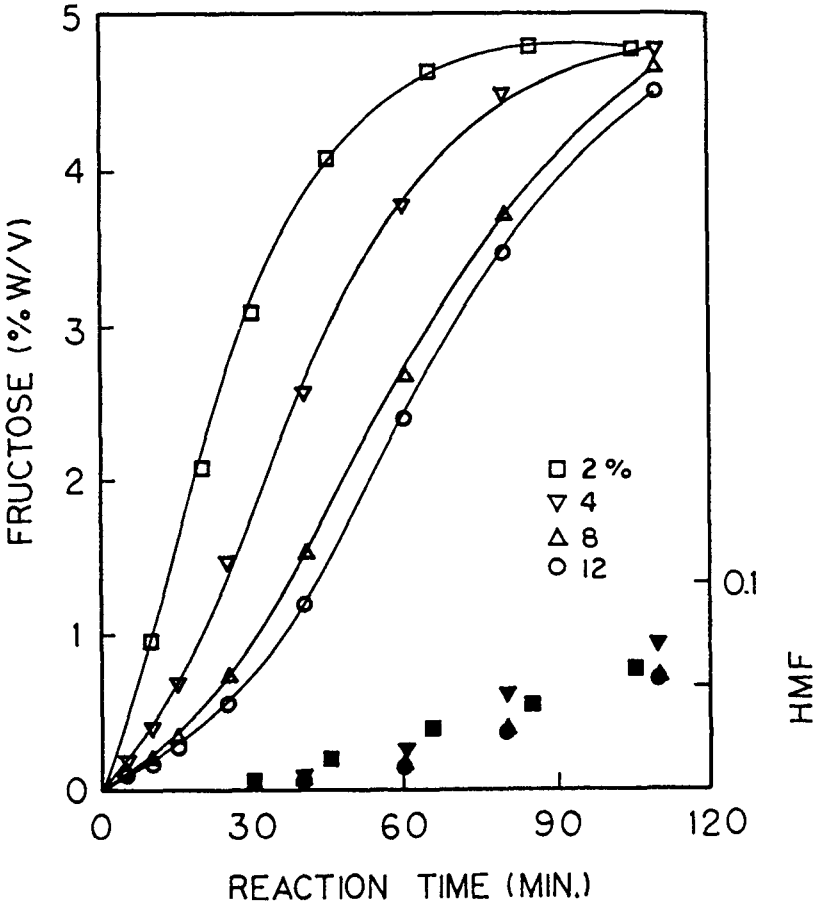

Fig. 3. Effect of crosslinkage on reaction rate (dry mesh size 50–100). Dowex 50W resins. Batch Reactor. 100°C. Catalyst Loading: 3 g/80 mL. Filled Symbols: HMF.

model previously described. The theoretical yield vs conversion for various Thiele modulus, ϕ, are shown in Fig. 4. The kinetic parameter, $S = k_1/k_2 = 100$, was chosen as a representative number applicable for inulin hydrolysis (see next section). This figure also gives a direct comparison between the performance of nonporous and porous catalyst. For nonporous catalyst, the yield of B is proportional to the conversion of A up to near complete conversion (because of high S value) and it is higher than the yields obtainable from porous catalysts. Figure 4, in essence, provides a theoretical proof that the effect of pore diffusion in a sequential reaction is such that the yield of the middle component is reduced when $k_1 > k_2$. To further verify this point, the kinetic constants were estimated using the data obtained from one of the earlier runs (Dowex 50Wx2-400, Fig. 2) and subjecting them to a statistical analysis based on SAS NLIN program (*18*). The resulting kinetic constants were: $k_1 = .0542$, $k_2 = .0006$ min^{-1}, thus $S = 90$. The experimental data were then put into the yield vs conversion plot and compared with the theoretical prediction (Fig. 5). The diffusivity ratio of $R_D = 50$ was taken from our experimental data (presented in the next section). The initial R_D value (diffusivity of fructose/diffusivity of fresh inulin) was actually determined to be about 100. This value, however, is expected to decrease as the reaction progresses, reaching unity at the completion of the reaction.

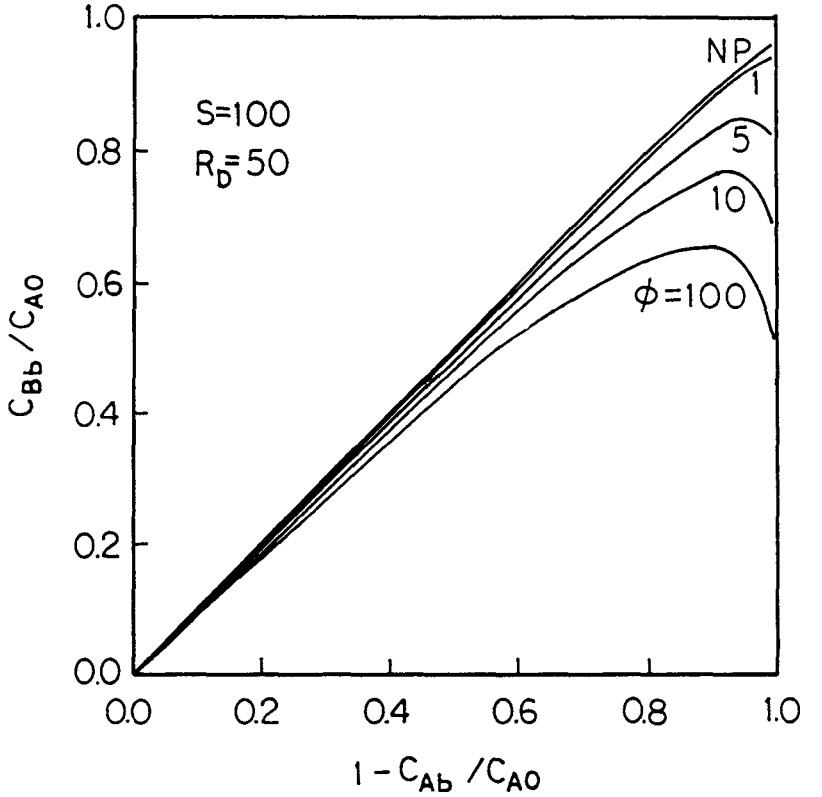

Fig. 4. Effect of intraparticle diffusion on yield of B for consecutive reaction (A→B→C). Unsteady state model. $S = k_1/k_2$, $R_D = De_B/De_A$.

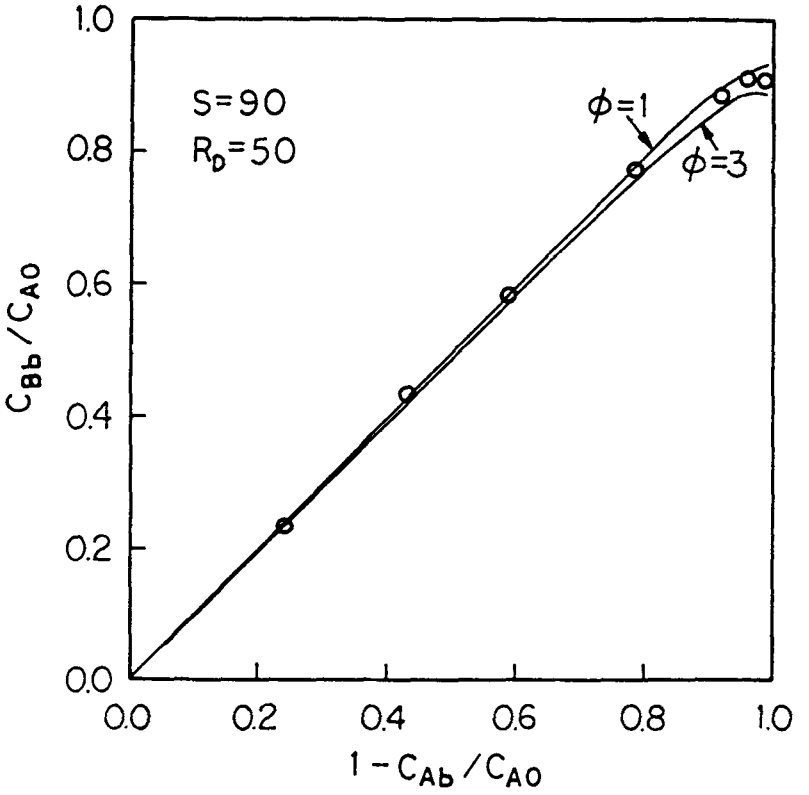

Fig. 5. Effect of intraparticle diffusion on fructose yield. Dowex 50x2-400. Experimental data (○). Model prediction (—).

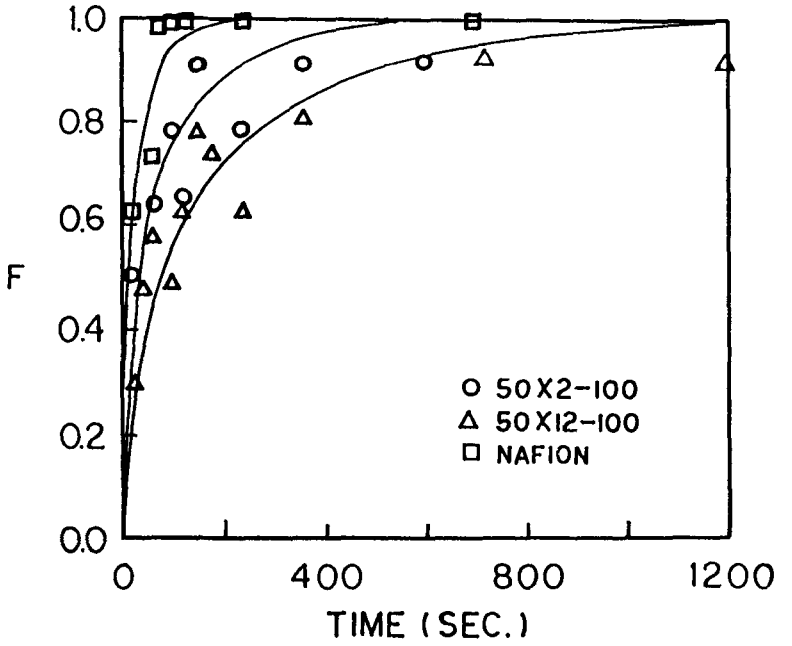

Fig. 6. Fractional uptake of fructose by various type of resins. —: Best-fit curve from statistical analysis.

Therefore the average value of 50 was taken in the calculation of the theoretical curve. Figure 5 shows that the experimental data points lie between the theoretical curves for which $\phi = 1$, and $\phi = 3$. This again indicates that the reaction is subject to significant diffusion limitation. Because of the small particle size and low degree of crosslinking (400 mesh, 2%), however, the reaction under the present condition was not totally controlled by diffusion, as indicated by the low magnitude of the Thiele modulus. The close fit between the theoretical curve and experimental data also confirms the validity of this model.

Diffusion in Resin Particle

For measurement of diffusivity of fructose within the resin, sorption tests were conducted using Dowex 50Wx2-100, 50Wx12-100, and Nafion. The sorption data indicated that the amount of fructose sorbed in Dowex 50Wx2-100 (2% crosslinking) is almost twice that in Dowex 50Wx12-100 (12% crosslinking) and four times that in Nafion (uncrosslinked). This implies that the crosslinkage (i.e., porosity) of an ion exchange resin significantly affects the sorption of fructose. Shown in Fig. 6 is the fractional uptake of fructose by various types of resins. The diffusivity was determined from the data of F vs time using SAS NLIN program (*18*). The first 10 terms of the infinite series solution (*17*) were considered. Also noticeable from this figure is that the fractional uptake for Nafion reached unity in less than 200 s. This could be explained by the fact that Nafion has very small void volume near the surface, consistent with the findings of Beltrame, et al. (*22*). The slightly increased activity of the finer catalyst could be attributed not to easier diffusion into pores, but to the actual increase in external surface area created by size reduction. In contrast to Nafion, the fractional uptakes in Dowex 50Wx2-100 and 50Wx12-100 leveled off at about .9, indicating that some of the pores in these resins are too small to accommodate fructose molecules.

The experimentally determined effective diffusivities of fructose are tabulated in Table 2. Diffusivity of fructose for Dowex 50Wx2-100 or Nafion is almost 4 times that for Dowex 50Wx12-100. The diffusivity of glucose in water has been reported to be 6.73×10^{-6} cm^2/s at 25°C (*23*). If the diffusivity of fructose is the same as that of glucose, the rate of diffusion in Dowex 50Wx2-100 or Nafion is about 1/5 of that in water. Although absolute comparison of diffusivities is difficult because of the differences in solute, resin, and temperature applied, the results found in

Table 2
Effective Diffusivities of Fructose and Inulin

	Diffusivity (cm^2/s)	
Catalyst	Fructose	Inulin
Dowex 50Wx2-100	1.4×10^{-6}	1.3×10^{-8}
Dowex 50Wx12-100	3.7×10^{-7}	—
Nafion	1.5×10^{-6}	—

this study are in close proximity of those reported in the literature (*24,25*). Effective diffusivity of inulin also was measured in Dowex 50Wx2-100 at 26°C. The fractional uptake of inulin by Dowex 50Wx2-100 was less than half that of fructose by the same resin. This would indicate that only macropores near the surface are available for inulin diffusion. The measured effective diffusivity of inulin (listed in Table 2) was found to be only one hundredth of that of fructose in the same resin.

Pseudo Steady State Model

From the results of effective diffusivities, it became clear that the sluggishness in reaction rate at the initial stage of reaction is caused by slow diffusion of the reactant. Initially, the fresh inulin of high DP exists in solution. However, as inulin is depolymerized, the diffusion rate of the reactant is progressively increased, consequently the reaction is accelerated. It is difficult to estimate the change of diffusivity corresponding

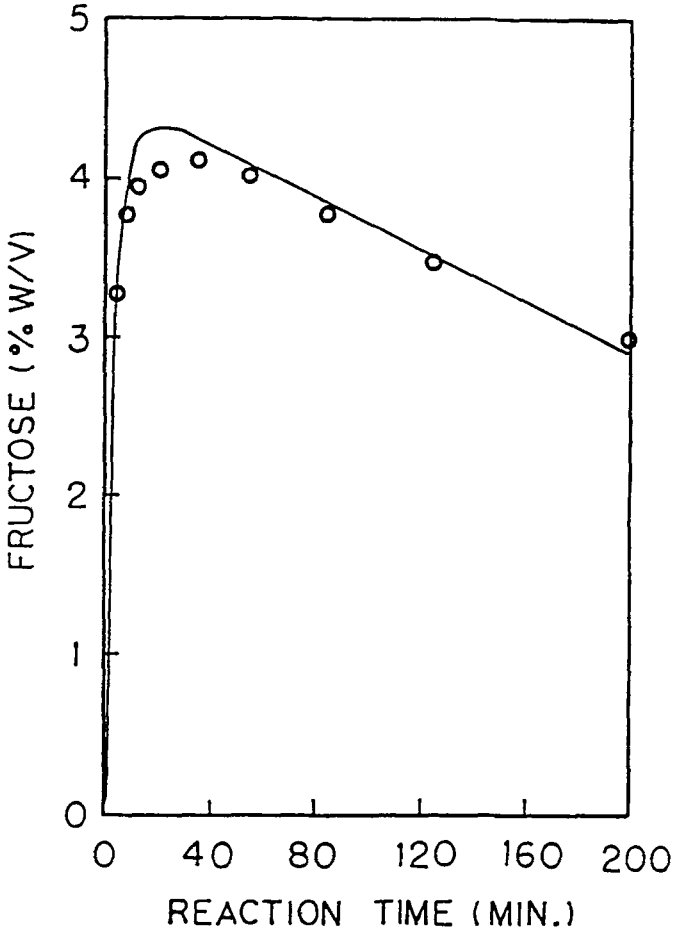

Fig. 7. Hydrolysis of inulin by .0398 N sulfuric acid. 100°C, —: Best-fit curve from statistical analysis.

to depolymerization. As an approximation and for calculation purpose, it was assumed that the effective diffusivity of reactant changes proportionally to the reaction conversion. Accounting such variation of diffusivity, the pseudo steady model equations of (*19*) and (*20*) were numerically solved simultaneously employing fourth order Runge-Kutta method to provide the theoretical prediction of the reaction progress as it is influenced by diffusion. For this purpose, the intrinsic kinetic constants were experimentally determined. In so doing, .0398 N H_2SO_4 which is equivalent to 3 g of Dowex 50Wx2-400/80 mL solution was used in place of the resin, since the smallest particle resin was still subject to strong diffusional effect. The reaction progression using sulfuric acid is shown in Fig. 7. The kinetic constants statistically determined from this run were: k_1 = .279, k_2 = .0022 min $^{-1}$, and they were used in the computation for the theoretical prediction. The results of these calculations are presented in Figs. 8 and 9, which are designed to show the effects of

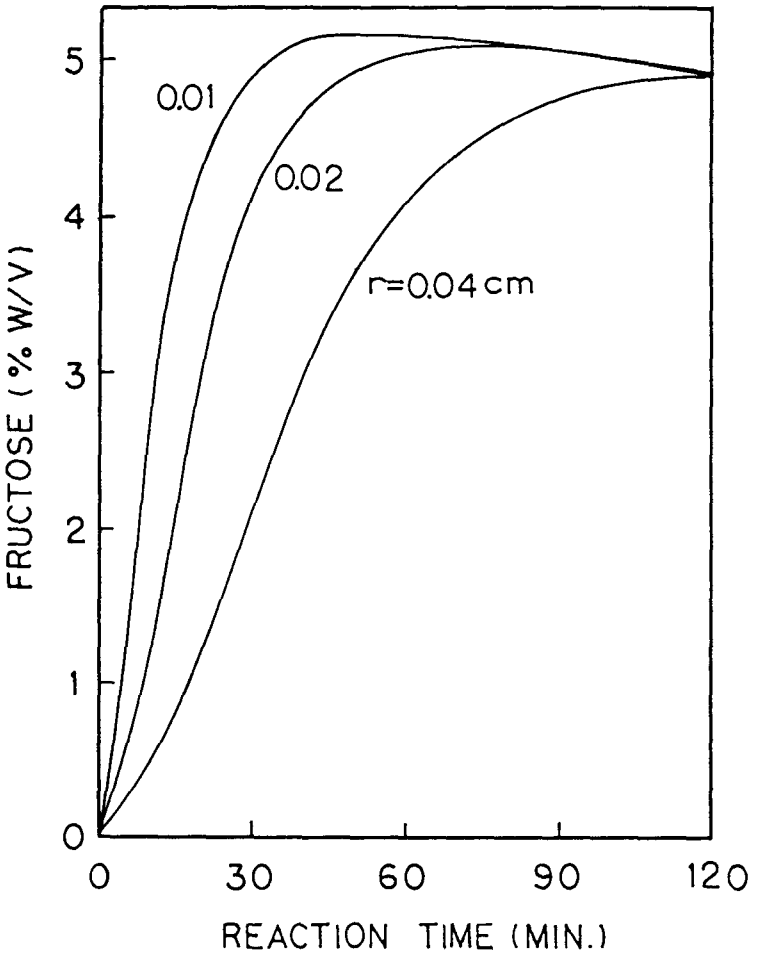

Fig. 8. Theoretical prediction on effect of particle size on reaction rate. Pseudo steady state model. (Porosity = .12, k_1 = .279, k_2 = .0022 min $^{-1}$)

particle size and porosity on the reaction rate and the pattern. As expected, the reaction rate increased with porosity, and decreased as the particle size increased. The accelerating reaction pattern at the early phase of the reaction has indeed appeared in this theoretical prediction, reflecting the gradual change of DP (thus the diffusivity). It is also proven that such reaction pattern is created solely as a result of the pore diffusion effect because the initial sluggishness in the reaction was totally absent in the run using sulfuric acid (Fig. 7), and it progressively diminished for small particle size and for large porosity (Figs. 8 and 9). Because of the assumptions made in this model, no attempts were made to fit the experimental data into the theoretical predictions. Nevertheless, this modeling work was found meaningful in that it provided a plausible explanation for the experimental observations of Figs. 1–3.

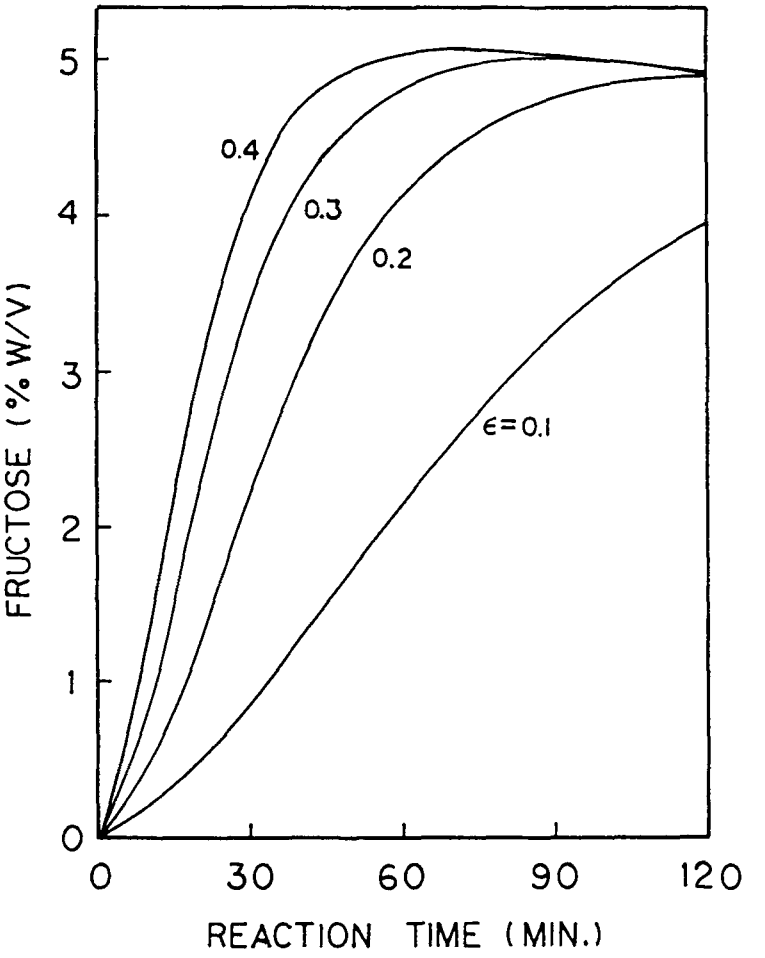

Fig. 9. Theoretical prediction on effect of porosity on reaction rate. Pseudo steady state model. (Particle size = .04 cm, k_1 = .279, k_2 = .0022 min^{-1})

CONCLUSIONS

The catalytic performance of several ion exchange resins was studied in connection with inulin hydrolysis. On the basis of specific reactivity and HMF formation, Dowex 50Wx2-100, Amberlite 200, and Nafion were found to be suitable for application in inulin hydrolysis. The particle size and porosity of the resin induced profound effects on the hydrolysis reaction, indicating that the intraparticle diffusion controls the reaction rate. The effective diffusivities of fructose and inulin were determined from the unsteady state sorption data. Theoretical models were developed to account for the effects of intraparticle diffusion. The results of unsteady model supported the experimental findings concerning the adverse effects of pore diffusion that it reduces the selectivity as well as the overall reaction rate. The results of pseudo steady state model provided a theoretical proof for the experimental observation that the pore diffusion effect creates an accelerating reaction pattern because of change of diffusivity during the hydrolysis reaction.

REFERENCES

1. Ylikahli, R. H., and Pelkonen, R. (1980), *Carbohydrate Sweeteners in Foods and Nutrition*, Academic, London.
2. Fleming, S. E., and GrootWassink, J. W. D. (1979), *CRC Critical Reviews in Food Science and Nutrition* **12,** 1.
3. Chubey, B. B., and Dorrell, D. G. (1974), *Can. Inst. Food Sci. Technol. J.* **7,** No. 2, 98.
4. Dykins, F. A., et al. (1933), *Ind. Eng. Chem.* **25,** no. 10, 1165.
5. Eichinger, J. W., et al. (1932), *Ind. Eng. Chem.* **24,** no. 1, 41.
6. Dykins, F. A., et al. (1933), *Ind. Eng. Chem.* **25,** No. 8, 937.
7. Zhong, S., et al. (1985), A Study of Acid-Catalyzed Hydrolysis of Jerusalem Artichoke Juice in an Autoclave, presented at the First International Conference on Jerusalem Artichoke and Other Bio-Energy Resources, Daejeon, Korea.
8. Helfferich, F. (1962), *Ion Exchange*, McGraw Hill, New York.
9. Kim, S. B., and Lee, Y. Y. (1985), *Biotechnol. Bioeng. Symp.* **1,** 81.
10. Levesque, C. L., and Craig, A. M. (1948), *Ind. Eng. Chem.* **40,** no. 1, 96.
11. Haskell, V. C., and Hammett, L. P., (1949), *J. Amer. Chem. Soc.* **71,** 1284.
12. Bodamer, G., and Kunin, R. (1951), *Ind. Eng. Chem.* **43,** no. 5., 1082.
13. Reed, E. W., and Dranoff, J., (1964), *I & EC Fundamentals* **3,** no. 4, 304.
14. Gilliland, E. R., et al. (1971), *I & EC Fundamentals* **10,** no. 2., 185.
15. MacBean, R. D., et al. (1979), *Austral. J. Dairy Technol.* p. 53.
16. Wheeler, A. (1951), *Advances in Catalysis* **3,** 250.
17. Crank, J. (1975), *The Mathematics of Diffusion*, Claredon, Oxford.
18. SAS User's Guide: Statistics (1982), SAS Institute, Cary, NC.
19. Rigal, L. et al. (1981), *Ind. Eng. Chem. Prod. Res. Dev.* **20,** 719.
20. Kunin, R. (1958), *Ion Exchange Resins*, Wiley, New York.
21. Dow Chemical Co. (1959), *Dowex: Ion Exchange*, Midland, MI.

22. Beltrame, P. et al. (1980), *Ind. Eng. Chem. Prod. Res. Dev.* **19,** 205.
23. Weast, R. C., ed. *Handbook of Chemistry and Physics,* F45, 65th edition, CRC Press, Boca Raton, FL.
24. Ghim, Y. S., and Chang, H. N. (1982), *I & EC Fundamentals* **21,** 369.
25. Yeo, S. C., and Eisenberg, A. (1977), *J. Appl. Polym. Sci.* **21,** 875.